Servolab Science News Vol.1(1): 60-70 (2022) 7 Figs. 1 Tab. 1 Scheme

REACTION OF 3-MERCAPTO-1-PROPANOL WITH ACRYLAMIDE ON GOLD SURFACES

(REACCIÓN DE 3-MERCAPTO-1-PROPANOL CON ACRILAMIDA SOBRE SUPERFICIES DE ORO)

NATALIA N. OLMEDA-VIERA[1], JENNIFER CAMACHO-LUGO[1], CORAL ALICEA-MAUNETO[1], ERIKA SERRANO-DÍAZ[1], ROSA D. BRITO-GÓMEZ[2], ROLANDO J. TREMONT[1]

[1] Department of Chemistry, University of Puerto Rico at Humacao, [2] Faculty of Sciences and Technology, Department of Natural Science, Interamerican University of Puerto Rico

E-mail: rolando.tremont@upr.edu

ABSTRACT

In this work we study the molecular structure formed by the reaction of 3-mercapto-1-propanol (3-MP) with acrylamide (AA) on gold surfaces, through of self-assembly technique. The first step was the formation of a self-assembled monolayer (SAM) of 3-MP on the gold surface, using a 3.0 mM solution in anhydrous ethanol. Then, this monolayer reacted with acrylamide using a 2.5 mM solution of AA in a slightly basic solution. These surfaces were characterized by cyclic voltammetry (CV), X-ray photoelectron spectroscopy (XPS), and FT-IR specular reflectance. By CV, 2.5 mM $Fe(CN)_6^{3-}$ solution as the redox active couple was used, in 0.10 M KCl solution. Increasing amount 3-MP and AA on the gold surface, the reduction and oxidation current of ferricyanide species become smaller, indicating a blockade of the surface. In the XPS study, the binding energy peaks of Au, C, O, S, and N were shown. In the 3-MP/Au surface the C, O, and S were presents. In the derivatized surface we obtained clear signals of C-O-C, C=O and $C-NH_2$. The results obtained by FT-IR specular reflectance showed different absorption bands for 3-MP, AA and after derivatization on the gold surface.

Keywords: SAMs; 3-mercapto-1-propanol; acrylamide, chemical derivatization, surface analysis.

RESUMEN

En este trabajo se estudia la estructura molecular sobre superficies de oro formada por la reacción de 3-mercapto-1-propanol (3-MP) con acrilamida (AA), mediante la técnica de autoensamblaje. El primer paso fue la formación de una monocapa autoensamblada (SAM, por sus siglas en inglés) de 3-MP sobre la superficie del oro, utilizando una solución 3,0 mM en etanol anhidro. Luego, esta monocapa reaccionó con acrilamida usando una solución 2,5 mM de AA en una solución ligeramente básica. Estas superficies se caracterizaron por voltamperometría cíclica (CV, por sus siglas en inglés), espectroscopía de fotoelectrón de rayos X (XPS, por sus siglas en inglés) y reflectancia especular FT-IR. Por CV, se utilizó una solución de ferricianuro ($Fe(CN)_6^{3-}$) 2,5 mM como el activo redox, en una solución de KCl 0,10 M. Al aumentar la cantidad de 3-MP y AA en la superficie del oro, la corriente de reducción y oxidación del ferricianuro se hacen más pequeñas, lo que indica un bloqueo de la super-

Reccived: 17/06/2021
Accepted: 02/12/2021

ficie. En el estudio de XPS, se mostraron los picos de energía de enlace de Au, C, O, S y N. En la superficie 3-MP/Au estaban presentes C, O y S. En la superficie derivatizada se obtuvo señales claras de C-O-C, C=O y C-NH_2. Los resultados obtenidos por reflectancia especular FT-IR mostraron diferentes bandas de absorción para 3-MP, AA y después de derivatización sobre la superficie del oro.

Palabras claves: SAMs; 3-mercapto-1-propanol; acrilamida, derivatización química, análisis de superficies.

INTRODUCTION

Acrylamide (AA) is a neurotoxic substance that is formed when we cook foods rich in sugars at high temperatures. This compound is formed when an amino acid reacts with a reducing sugar. (Tateo *et al*. 2010; Anese *et al*. 2011). This substance is present in coffee, chips, cookies, and cereals (Andrzejewski *et al*. 2004; Taeymans *et al*. 2005). The risks of developing cancer and genetic mutations have been proven in animal studies in research laboratories (Von Mühlendahl & Otto 2003; Törnqvist 2005; Capuano & Fogliano 2011). This compound has been classified as a chemical producer with carcinogenic potential and has been included in category 2. Until now, the minimum concentration to be considered dangerous in the human body is not known, although it is not cumulative and is discarded by the body.

The determination of acrylamide in foods has been done by several analytical techniques, including capillary electrophoresis, high performance liquid chromatography, gas chromatography and electrochemistry. The most used technique is high performance liquid chromatography and mass spectroscopy (Dunovská *et al*. 2006; Keramat *et al*. 2011; Tekkeli *et al*. 2012; Vesela & Sucman 2013; Yoshioka *et al*. 2020).

The self-assembly technique allows us to form ordered monolayers of molecules on the metal surface, by adsorption. This allows us to obtain well-defined molecular structures on solid surfaces (Krajewska *et al* 2008). The formation of these organized surfaces allows us to react on them, to be used in molecular recognition on a well-ordered surface (Allara & Unozo 1985; Finklea *et al*. 1986; Swalen *et al*. 1987; Chidsey & Loiacono 1990; Laibinis *et al*. 1991; Finklea & Hanshew 1992; Finklea *et al*. 1993; Ulman 1996; Krajewska *et al*. 2008).

This work is focused on the study of the reaction of 3-MP with AA on gold surfaces using spectroscopic and electrochemical techniques. SAM of 3-MP on gold surfaces was prepared successfully. This reaction was followed by CV, XPS and FT-IR. This new system can serve to recognize the acrylamide compound in aqueous solution.

MATERIAL AND METHODS

Chemicals

Potassium ferricyanide ($K_3Fe(CN)_6$) (Aldrich, 99%), 3-mercapto-1-propanol ($HSCH_2CH_2CH_2OH$, 3-MP) (Aldrich, 99%), acrylamide ($H_2NCOCHCH_2$, AA) (Aldrich, 99%), potassium chloride (KCl), ethanol Anhydrous (Aldrich, 99.8), sulfuric acid (Aldrich, 99.999%), sodium hydroxide (NaOH, 99%), were used as received. The water used was previously distilled and pumped through a nanopure system (Barnstead) to give 18 MW-cm water. All electrochemical measurements were done at room temperature. The aqueous solutions were degassed with nitrogen for least 30 min prior to an electrochemical experiment.

Cell and instrumentation

The electrochemical cell employed was a conventional three-electrode cell using platinum wire as a counter electrode. All potentials are reported with respect to Ag/AgCl reference electrode. A potentiostat/galvanostat EC Epsilon from BASi, connected to a cell stand C-3 for voltammetry. The cell is equipped with a platinum wire auxiliary electrode (7.5 cm) with gold-plated connector (MW-1032), and a 7.5 cm long RE-5B Ag/AgCl reference electrode with a Vycor frit (the filling solution is aqueous 3 M NaCl that has been saturated with AgCl). Software: EC epsilon version 1.60.70, were used.

X-ray photoelectron spectroscopy (XPS) was done using a PHI 5600ci spectrometer with an Al Ka X-ray source at 15 kV and 350 W. The pass energy used was 93 eV for the survey analysis and 59 eV for high energy resolution studies.

The binding energy values reported were corrected using the C 1s signal of the atmospheric contaminants (285.0 eV).

For FT-IR studies a 100 FTIR Spectrometer, from Perkin Elmer, equipped with a Universal ATR (uATR) top plate accessory one refraction. Software: Spectrum version V.6.0, was used.

Substrate pre-treatment

A cleaning treatment was applied to the gold surfaces used, before being modified. The polycrystalline gold electrodes used for the electrochemical measurements were prepared by polishing gold electrodes with 1.0, 0.3, and 0.05 mm Al_2O_3 paste, and then rinsed copiously with nanopure water. Before the modification and derivatization, the cleaning of the electrodes was verified by cyclic voltammetry in a 1.0 M H_2SO_4 solution until the characteristic CV was observed. The electrode was polished with Al_2O_3 paste, again and washed copiously with nanopure water. Finally, they were dried with an argon gas flow. A cyclic voltammogram of a clean gold electrode of 1.6 mm of diameter in 1.0 M H_2SO_4, at 100 mV/s scan rate is shown in **Fig. 1**. The current-potential behavior shown in this figure is characteristic of a clean Au surface in a clean test solution (MACDONALD & JOHNSON 1987; LAIBINIS *ET AL*. 1992; TOGNI & HAYASHI 1995; XING *ET AL*. 2003).

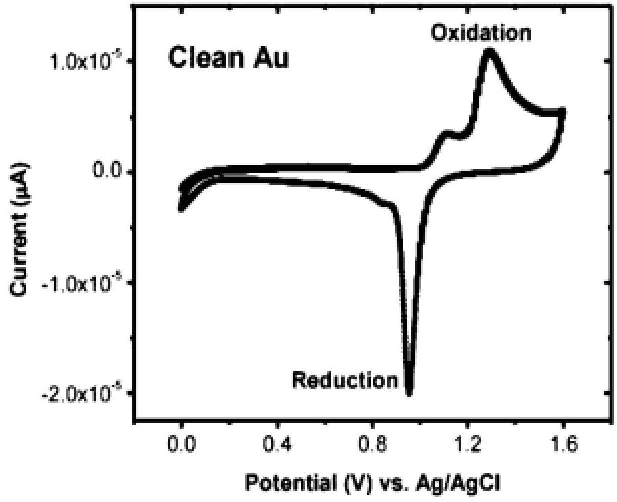

Figure 1. Cyclic voltammogram of clean gold surface in 1.0 M H_2SO_4 solution. Scan rate 100 mV s^{-1}. The solution was degassed with N_2 flow for least 30 min. Measurements were performed at 21 ± 1 °C.

Preparation of self-assembled of 3-MP on gold surfaces

MAXTEK$^{\text{â}}$ gold substrates were used for the surface study. These crystals are composed of 2000 Å of gold on top of a polished AT-cut quartz crystal, using a thin film of chromium or titanium as an underlayer to improve adhesion between gold and the quartz crystal.

Commercial gold disk electrodes (Bio-Analytical System, BAS) of 1.6 mm of diameter were used to carry out the electrochemical study.

The previously cleaned substrates were submerged in a 3.0 mM 3-MP ethanol solution for 24 hours, for surface studies.

Derivatization of the SAMs of 3-MP/Au

The surface modified with 3-MP, was exposed to an AA solution for its derivatization. The reaction was carried out in 2.5 mM AA, in a slightly basic solution, for 48 hours. After this step, the AA/3-MP/Au surface was removed from this solution, rinsed with ethanol, dried with argon and placed in a desiccator to be characterized. **Scheme 1** shows the complete process of modification and reaction on gold surfaces.

RESULTS AND DISCUSSION

Electrochemical studies

To study the modified gold surface with a 3 MP monolayer, the cyclic voltammetry (CV) technique was applied. With this technique it is possible to demonstrate that the gold surface has been modified with this molecule. 2.5 mM of $Fe(CN)_6^{3-}$, in 0.10 M KCl solution, was used to characterize these modified surfaces. The electrochemical responses of $Fe(CN)_6^{3-}$ on these surfaces are shown in **Fig. 2**, corresponding to (a) for clean gold, (b) gold surface modified with 3.0 mM 3-MP for 24 hours, in alcoholic solution (3-MP/Au) and (c) 3-MP/Au surface derivatized with 2.5 mM acrylamide (AA) for 48 hours, in a slightly basic solution. It was noted that the increasing number of organic molecules on gold surface bring as consequence a diminution of the peak current of the reduction and oxidation of ferricyanide species, indicating a blockade of the surface.

The electrochemical responses are clear and an important difference between peak currents of the unmodified and modified surface is observed. The answer in **Fig. 2 (c)** is due to the derivatization achieved on the surface. A possible explanation for this current may be that the molecules are relatively small. Another explanation is the possible presence of active sites on the gold surface, which could be causing current responses to be observed, without the surface being completely blocked. A similar voltammetric behavior was found previously with modified platinum electrodes with 3 mercaptopropionic acid (HSC_2H_4COOH) and 3-aminopropyltrimethoxysilane ($H_2NC_3H_6Si(OCH_3)_3$) (Laibinis *et al.* 1992; Togni & Hayashi 1995).

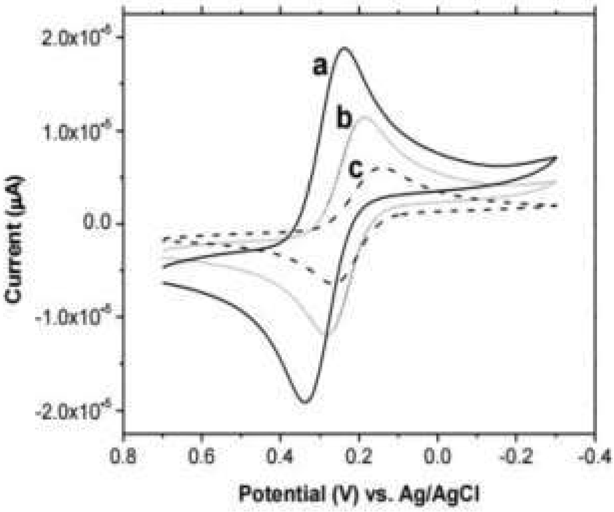

Figure 2. Cyclic voltammograms of 2.5 mM $K_3Fe(CN)_6$ in 0.10 M KCl solution: (a) for clean gold, (b) gold surface modified with 3.0 mM 3-MP for 24 h (3-MP/Au) and (c) 3-MP/Au surface derivatized with 2.5 mM acrylamide solution for 48 h. Scan rate 100 mV s^{-1}. Measurements were performed at 21 ± 1 °C.

Spectroscopic characterization.

X-ray photoelectron spectroscopy (XPS) studies

X-ray photoelectron spectroscopy (XPS) has been widely used to study the composition of self-assembled thiols. For example, Laibinis *et al.* (1992) studied the structure and composition of different *n*-alkanethiols on copper, silver, and gold surfaces. In this work, we performed XPS measurements to study the composition of 3-MP/Au SAM and AA/3-MP/Au derivatized on gold surfaces at take-off angle of 45 degrees. The survey XPS spectra of the gold substrate untreated (blank) and treated with 3 mM 3-MP, in ethanolic solution for 24 hours, afterward derivatized with AA, are shown in **Fig. 3** (A, B, and C).

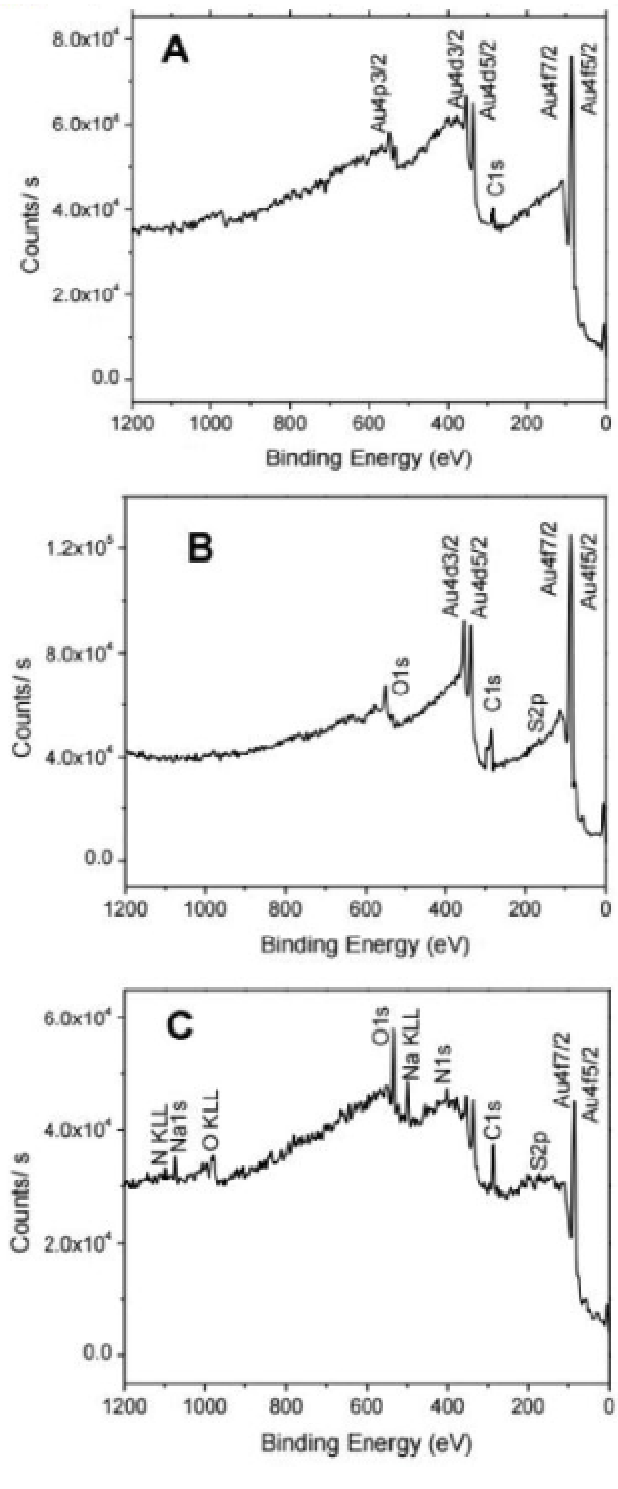

Figure 3. XPS spectra of the (A) bare Au, (B) 3-MP/Au, and (C) AA/3-MP/Au electrode systems.

These spectra showed photoemission peaks that were attributed to the Au, C, O, N, and S atoms that are present in the 3-MP and AA modified gold surface. The spectra in **Fig. 3A** present the binding energy peaks that were attributed to the *Au* ($4f_{7/2}$ and $4f_{5/2}$) and C1s, which are present at the gold clean. The presence of carbon is attributable to environmental pollution. The blank XPS spectrum, shown in **Fig. 3A**, has the same XPS signals as that presented for the Au modified surfaces, with exception of the S2p and O1s signals (**Fig. 3B**). The modification of the gold surfaces with 3-MP is confirmed with the S binding energy peaks. **Fig. 3C** shows the presence of C1s and O1s with greater intensity than in **Figs. 3A and 3B**. It also shows N1s. In addition to the above signals, the presence of sodium is shown, because it was part of the aqueous solution where the derivatization reaction occurred, being trapped in the monolayer (LAIBINIS *ET AL.* 1992; YANG *ET AL.* 2001).

XPS spectra for the core binding energy region of gold are shown in **Fig. 4**. The three spectra, taken under the same instrumental conditions, reveal how the signal of gold is reduced when the Au surface is modified with 3-MP (**Fig. 4Ab**) and derivatized with AA (**Fig. 4Ac**). The decrease on the peak height and area is an indication that these compounds are adsorbed on the Au surface and are blocking the XPS detection of Au 4f photoelectrons.

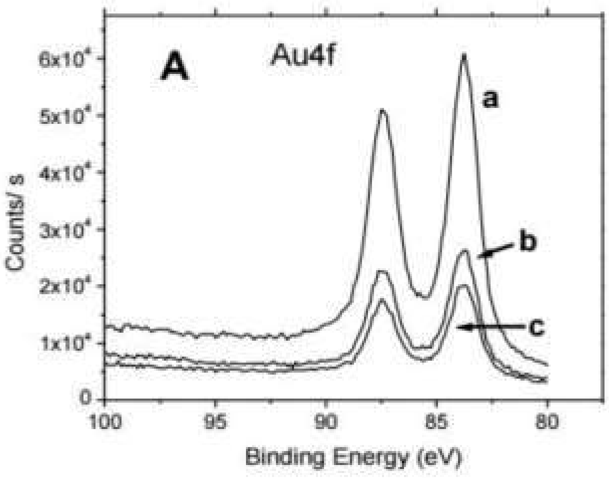

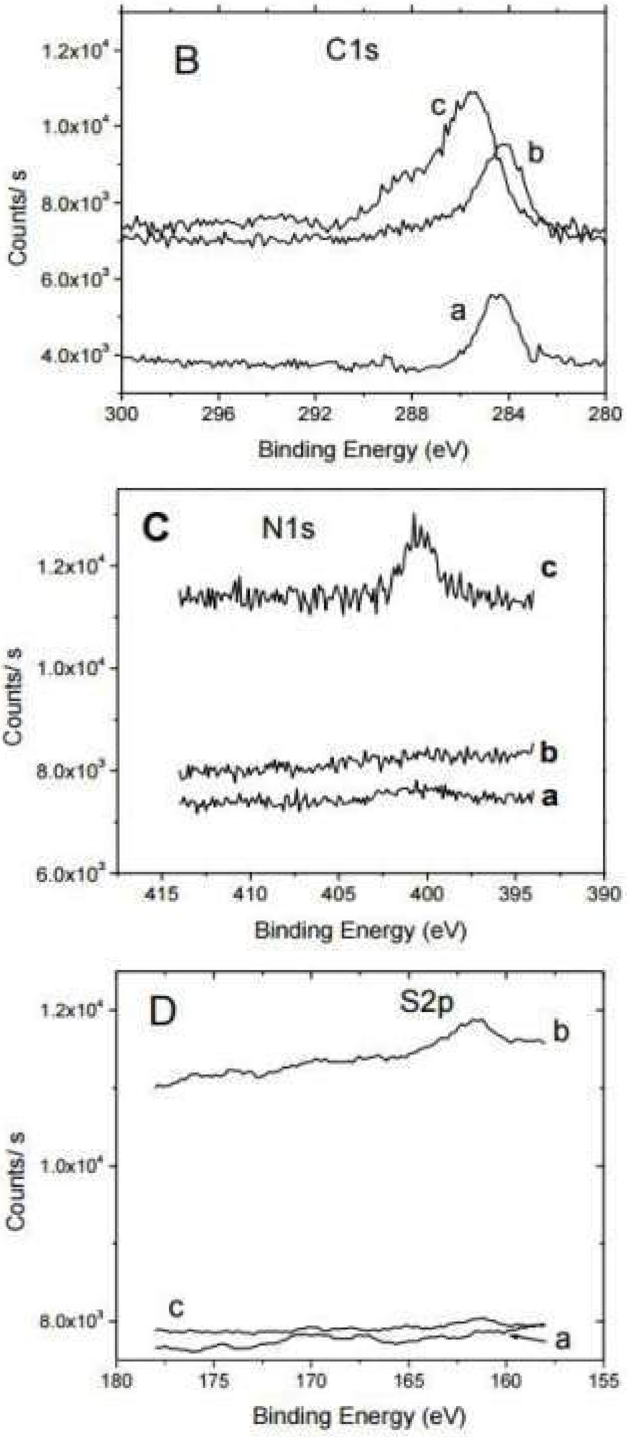

Figure 4. High-resolution XPS spectra for (A) the $Pt4f_{5/2}$ and $Pt4f_{7/2}$ core binding energy region: (a) bare Au, (b) 3-MP/Au, and (c) AA/3-MP/Au electrode systems; (B) XPS spectra for C1s binding energy region: (a) bare Au, (b) 3-MP/Au, (c) AA/3-MP/Au electrode systems; and (C) (a) bare Au, (b) 3-MP/Au, and (c) AA/3-MP/Au electrode systems. Same XPS instrumental analysis conditions were used.

Fig. 4B shows the C1s region, where is observed that the greatest displacement in binding energy is shown by the AA/3-MP/Au surface (**Fig. 4Bc**), presenting a wide peak, where it can deduce several types of carbon on this surface. Figure 5 shows the high resolution XPS to assign the binding energies for each type of carbon, by functional groups.

Fig. 4C shows the N1s region, where the presence of nitrogen in the derivatized surface (**Fig. 4Cc**) is clearly observed. On the others surfaces, only noises were observed, discarding presence of nitrogen.

Fig. 4D shows the S2p region. The presence of sulfur on the surface of 3-MP/Au (**Fig. 4Db**) is clearly observed. The sulfur signal is attenuated on the AA/3-MP/Au surface because the sulfur atom forms a thiolate with the gold surface and the detection of its electrons are blocked by the derivatized molecules (**Fig. 4Dc**).

The chemical derivatization of the 3-MP/Au, with acrylamide, AA, was followed. **Fig. 5** (A, B, and C) shows curve-fitted high-resolution XPS spectra of this derivatization. The C (1s) binding energy region, for the AA/3-MP/Au surfaces (**Fig. 5A**), three peaks are observed. One peak at 287.7 eV, this peak can be attributable to N–C=O, the peak at 286.4 eV attributable to C-O-C, and the peak at 284.6 eV attributable to -CH_2 (Allara & Unozo 1985; Finklea *et al.* 1986; Swalen *et al.* 1987).

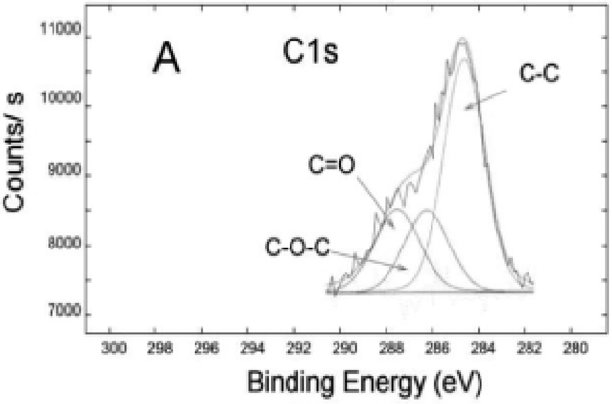

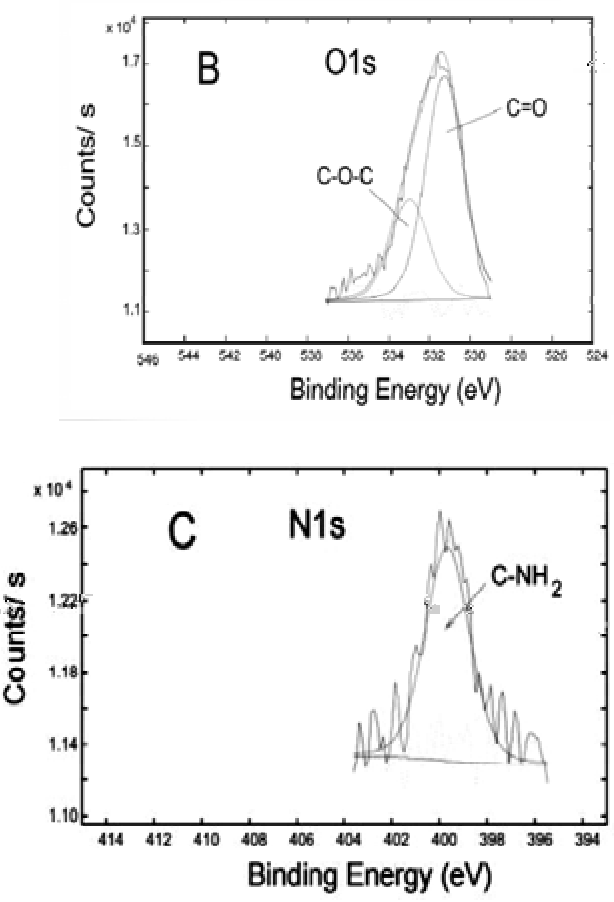

Figure 5. Curve-fitted high-resolution XPS spectra for (A) C1s, (B) O1s, and (C) N1s regions of AA/3-MP/Au electrode system.

Fig. 5B shows the curve-fitted high-resolution XPS spectra obtained for O1s. Here we observe two signals for O1s, one peak at 531.6 eV assigned at –C=O and 532.7 assigned at C-O-C (Chidsey & Loiacono 1990; Finklea & Hanshew 1992; Finklea *et al.* 1993).

XPS spectrum obtained of the N1s region, only one peak was observed at 400 eV (See **Fig. 5C**), attributable at -NH_2, this observation indicates the presence of amide bonds on the modified gold surface.

The atomic composition of C, O, Au, N and S, for each surface under study is shown in **Table 1**. The C1s signal for the AA/3-MP/Au surface is maximum. The presence of O1s on the 3-MP/Au and AA/3-MP/Au surfaces, is evident. The S2p signal on the 3-MP/Au surface is clearly seen, while it is almost imperceptible for the AA/3-MP/Au surface.

The atomic ratio of carbon to oxygen was calculated from XPS spectrum after each treatment at Au surface. The atomic ratio of C1s/O1s is 3.4 (3:1 for 3-MP/Au and 6:2 for AA/3-MP/Au). The atomic ratio of C1s/N1s is 6.3 (6:1). In these atomic composition ratios, an amount of carbon coming from atmospheric contaminants is observed.

Element	Clean Au (Atomic %)	3-MP/Au (Atomic %)	AA/3-MP/Au (Atomic %)
C1s	19.8	52.9	60.4
O1s	< 0.1	15.5	17.7
Au4f	80.2	19.6	11.4
N1s	0.0	0.0	9.6
S2p	0.0	12.0	0.9

Table 1. Atomic composition (%) on the different Surface from XPS analysis.

The organization of AA/3-MP on Au surface was studied by angle resolved X-ray photoelectron spectroscopy (ARXPS). As the take-off angle decreases, the surface sensitivity of XPS increases (Ratner *et al.* 1997; Brito *et al.* 2004). From angle-resolved XPS measurements, the AA/3-MP organization on gold surfaces at 15°, 30°, 45°, 60°, and 75° take-off angles was obtained. The relative presence for Au4f, at five different take-off angles, to derivatized gold surfaces (AA/3-MP) is shown in **Fig 6a**. It is observed that the relative presence of the substrate was increasing as the take-off angle was decreased. Since, the take-off angle was moved away of the surface and increased the sensitivity in depth, greater amount of the substrate is detected. The sulfur intensity decreased at greater angles (**Fig. 6b**). On the other hand, the carbon intensity decreased at 75° (**Fig. 6c**). These results indicate that the 3-MP compound have been adsorbed on the gold surface, through the sulfur. This demonstrates the diminution in the carbon intensity and the high presence of N1s (**Fig. 6d**) to greater angles. The amount of oxygen on the surfaces as the angle changes is shown in **Fig. 6e**. The -OH functionality (from 3-MP) being exposed in the film-solution interface has been derivatized, forming $O=C\text{-}NH_2$. Now, the amide will be present in the surface.

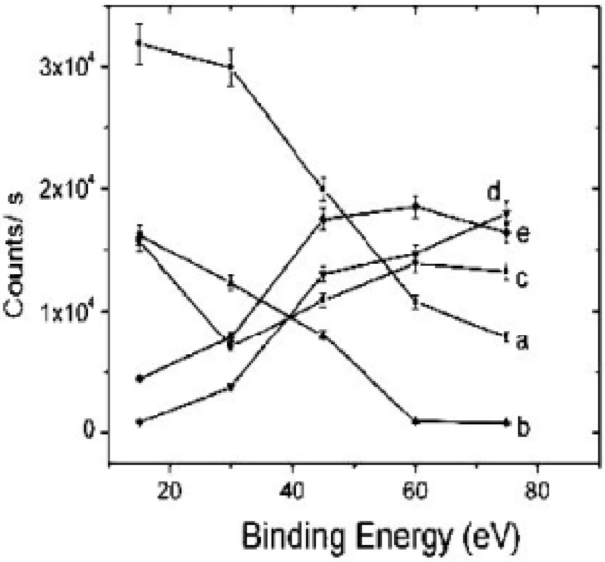

Figure 6. X-ray photoelectron angle resolved measurements for gold surface derivatized with acrylamide. Relative presence for (a) Au4f; (b) S2p; (c) C1s; (d) N1s; (e) O1s.

Infrared Spectroscopy Study

Infrared spectroscopy was another useful tool for studying the processes of chemical transformations on the gold surface. Figures 7A and 7B show the 3-MP and AA spectra, respectively. In the **Fig. 7A** can be observed absorption bands characteristics of the 3-MP. For example, the bands at 3350 cm^{-1}, 2480 cm^{-1}, and 1080 cm^{-1} corresponding to the stretch -OH, -SH, and -C-O, respectively. In the **Fig. 7B** absorption bands at 3369 cm^{-1} and 3177 cm^{-1} corresponding to the stretch $\text{-}NH_2$ can be appreciated. Also, the absorption band corresponding to the stretch -C=O of the acrylamide appear at 1661 cm^{-1}. Finally, the absorption band at 1600 cm^{-1} can be assigned to the C=C stretch conjugated of the acrylamide (Park & Kim 2010).

On the other hand, the IR spectrum of the gold surface derivatized with 3-MP and AA is shown in **Fig. 7C**. Some changes can be observed when this spectrum is compared with the spectra in **Figs. 7A and 7B**. For example, the disappearance of the absorption band at 2480 cm^{-1} (n-SH) is indicative that the 3-MP is adsorbed on the gold surface in the first step of the modification reaction forming $Au\text{-}S(CH_2)_3OH$ SAMs (**Scheme 1**). Other important fact is the disappearance of the stretch C=C at 1600 cm^{-1} of the AA. In this case an absorption band at 1092 cm^{-1} is appreciated. This band is attributed to the stretch C-O-C of the ether group that can be formed when the -OH group of the 3-MP and the double bond of the AA react in the final step of the derivatization on gold surfaces. The displacement of the stretch -C=O of AA from 1661 cm^{-1} to 1667 cm^{-1} is also be observed. This can be attributed to the effect of the derivatization reaction on gold surfaces in the final step of the reaction. The double bond of acrylamide is electron-deficient and produces Michael-type addition reactions, many of which are reversible. In general, the greater the nucleophilic character of the species it attacks, the faster the reaction will be. Compounds including a hydroxyl group, such as alcohols and phenols, react rapidly with the acrylamide in the presence of a base to form the corresponding ethers $ROCH_2CH_2CONH_2$ (Park & Kim 2010).

These results corroborate the modification of the Au surface and the derivatization achieved with AA, presented in the **Scheme 1**.

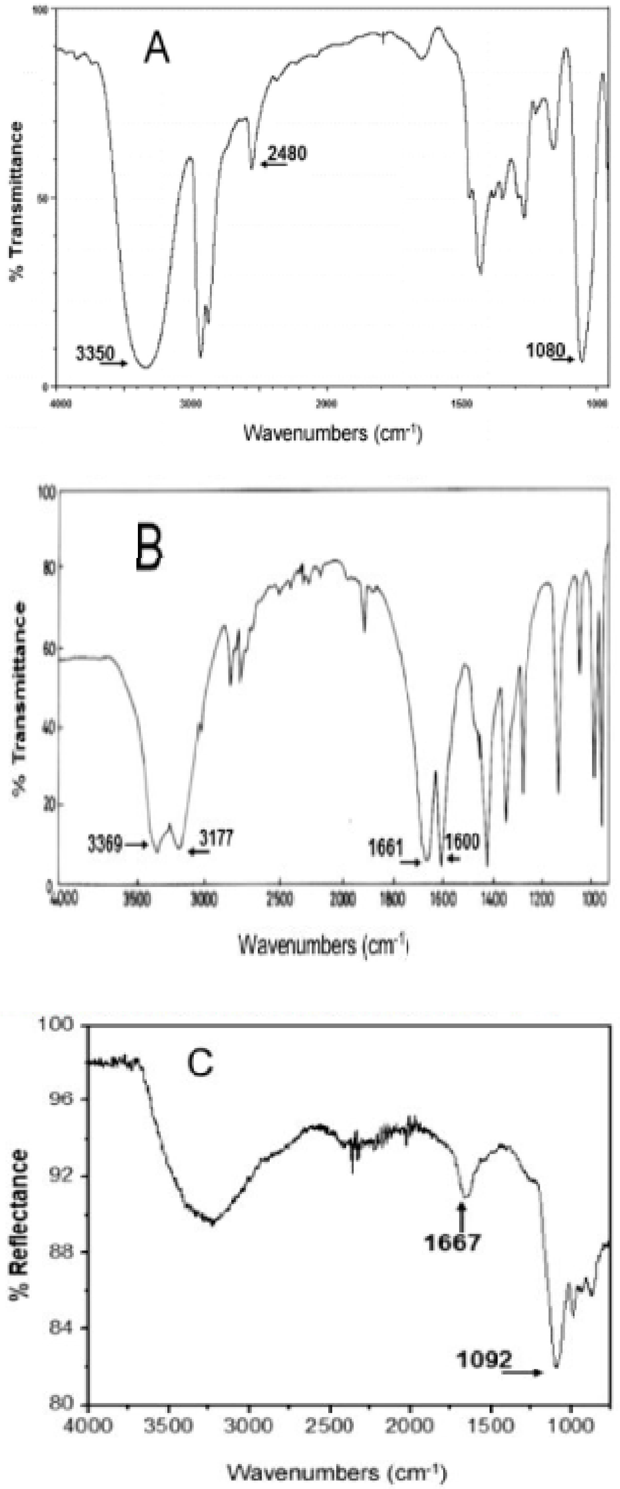

Figure 7. FT-IR spectrum of: (A) 3-mercapto-1-propanol (3-MP); (B) acrylamide (AA); (C) gold electrode derivatized with 3-mercapto-1-propanol and acrylamide measured by specular reflectance.

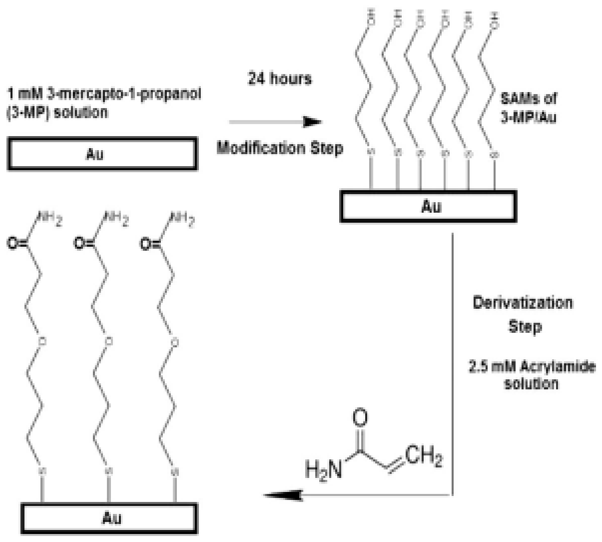

Scheme 1. Complete process of modification and reaction on gold surfaces.

CONCLUSIONS

The reaction of a-b unsaturated double bond of an amide, as in AA, with a surface that presents SAMs of 3-MP/Au (see **Scheme 1**) is a versatile and synthetically convenient method to generate derivatized surfaces that can be used to study the processes of adsorption. The derivatization of 3-MP/Au systems through Michael Addition reaction is a general procedure for inserting a wide variety of functionalities into modified surfaces. The cyclic voltammetry results indicate that the derivatized gold surfaces, compared with the modified gold surfaces, is most free of mass transfer effects. The spectroscopic analysis showed evidence of the process of chemical transformation on gold surface. XPS analyses indicated that the 3-MP and AA modified and derivatized the gold surfaces, respectively. These analyses also demonstrate the derivatization or conversion of the hydroxyl groups, of 3-MP, to ether groups when AA react with 3-MP, through Michael addition reaction. On the other hand, from the IR specular reflectance studies it was possible to corroborate the results obtained by XPS.

ACKNOWLEDGEMENTS

The authors would like to acknowledge the financial support of the Puerto Rico-Louis Stokes Alliance for Minority Participation (PR-LSAMP) Program, Maximizing Access to Research Careers (MARC-USTAR) Program, the use of facilities of the Materials Characterization Center of the University of Puerto Rico and the collaboration of Dr. Ramonita Diaz-Ayala with the XPS analyses. Also acknowledge the use of Department of Chemistry equipment's, University of Puerto Rico, Humacao Campus.

BIBLIOGRAPHIC REFERENCES

Allara D. L. & Nuzzo G. R. (1985). Spontaneously organized molecular assembled, Part 1. Formation, dynamics, and physical properties of n-alkanoic acids adsorbed from solution on an oxidized aluminum surface. *Langmuir*. 1: 45-52.

Andrzejewski D., Roach J. A., Gay M. L. & Musser S. M. 2004. Analysis of coffee for the presence of acrylamide by LC-MS/Ms. *J. Agric. Food Chem*. 52 (7): 1996-2002.

Anese M., Quarta B. & Frias J. M. 2011. Modelling the Effect of Asparaginase in Reducing Acrylamide Formation in Biscuits. *Food Chem*. 126 (2, 15): 435-440.

Brito R., Tremont R. Cabrera, C. & R. 2004, Electron transfer kinetics across derivatized self-assembled monolayers on platinum: a cyclic voltammetry and electrochemical impedance spectroscopy study. *J. Electroanal. Chem.* 574: 15-22.

Capuano E. & Fogliano V. 2011. Acrylamide and 5-hudroxymethylfurfural (HMF): A review on metabolism, toxicity, occurrence in food and mitigation strategies. *LWT-Food Sci. Science Technol*. 44: 793-820.

Chidsey C. E. D. & Loiacono D. N. 1990, Chemical functionality in self-assembled monolayers: structural and electrochemical properties. *Langmuir*. 6 (3): 682-691.

Dunovská L., Èajka T., HAJŠLOVÁ J. & Holadová K. 2006. Direct determination of acrylamide in food by gas chromatography-high-resolution time-of-flight mass spectrometry. *Anal. Chim. Acta*. 578: 234-240.

Finklea H. O. & Hanshew D. D. 1992. Electron-transfer kinetics in organized thiol monolayers with attached pentaamine (pyridine)ruthenium redox centers. *J. Am. Chem. Soc.* 114 (9): 3173-3181.

Finklea H. O., Ravenscroft M. S. & Snider D. A. 1993. Electrolyte and temperature effects on long range electron transfer across self-assembled monolayers, *Langmuir*. 9(1): 223-227.

Finklea H. O., Robinson L. R., Blackburn A., Richter B., Allara D. L. & Bright T. 1986. Formation of an organized monolayer by solution adsorption of octadecyltrichlorosilane on gold: electrochemical properties and structural characterization. *Langmuir*. 2 (2): 239-244.

Keramat J. Lebail A., Prost C. & Soltanizadeh N. 2011. Acrylamide in foods: chemistry and analysis. *Food Bioprocess Technol*. 4 (3): 340-363.

Krajewska A., Radecki J. H. & Radecka H. 2008. A voltammetric biosensor based on glassy carbon electrodes modified with single-walled carbon nanotubes/hemoglobin for detection of acrylamide in water extracts from potato crisps. *Sensors*. 8(9): 5832-5844.

Laibinis P. E., Nuzzo R. G. & Whitesides G. M.

1992. Structure of monolayers formed by coadsorption of two n-alkanethiols of different chain lengths on gold and its relation to wetting. *J. Phys. Chem.* 96: 5097-5105.

Laibinis P. E., Whitesides G. W., Allara D. L., Y. Tao T., Parikh Y. T. & Unozo R. G. 1991. Comparison of the structures and wetting properties of self-assembled monolayers on n-alkanethiols on the coinage metal surfaces Cu, Ag, Au. *J. Am. Chem Soc.* 113: 7152-7167.

Macdonald J. R. & Johnson, W. B. 1987. Impedance spectroscopy. Wiley, New York.

Park S. J. & Kim K. S. 2010. Surface characterization of carbon materials by X-ray photoelectron spectroscopy, Microscopy, in: A. Méndez-Vilas, J. Díaz (Eds.), Microscopy: Science, Technology, Applications and Education, Formatex.

Ratner B. D. & Castner D. G., in Vickerman, J. C. (ed.). 1997. Surface analysis, John Wiley & Sons, New York, Chap. 3.

Swalen J. D., Allara D. L., Andrade J. D., Chandross E. A., Garoff S., Israelachvili J., McCarthy T. J., Murria R., Pease R. F., Rabolt J. F., Wyanne K. J. & Yu H. 1987, Molecular monolayers and films. *Langmuir.* 3: 932-950.

Taeymans D., Andersson A., Ashby P., Blank I., Gonde P., van Eijck V. & Faivre S. 2005. Acrylamide: update on selected research activities conduced by the european food and drink industry. *J. AOAC Int.* 88: 234-241.

Tateo F., Bononi, M. & Gallone, F. 2010. Acrylamide content in potato chips on the Italian market determined by liquid chromatography tandem mass spectrometry. *Int. J. Food Sci. Technol.* 45 (3): 629-634.

Tekkeli S. E. K., Onal C. & Onal A. 2012. A review of current methods for the determination of acrylamide in food products. *Food Anal. Methods.* 5: 29-39.

Togni A. & Hayashi T. 1995. Ferrocenes: Homogeneous catalysis, organic synthesis, material science. VCH, New York.

Törnqvist M. 2005. Acrylamide in Food: The Discovery and Its Implications, in: Friedman, M. & Mottram, D. (eds.), Chemistry and Safety of Acrylamide in Food. *Adv. Exp. Med. Biol.* 561: 1-19.

Ulman A. 1996. Formation and structure of self-assembled monolayers. *Chem. Rev.* 96(4): 1533-1554.

Vesela H. & Sucman E. 2013. Determination of acrylamide in food using adsorption stripping voltammetry. *Czech J. Food Sci.* 31 (4): 401-406.

Von Mühlendahl K. E. & Otto M. 2003. Acrylamide: more than just another food toxicant?, *Eur. J. Paediatr.* 162: 447-468.

Xing Y. F., O'Shea S. J., & S. Li F. Y. 2003. Electron transfer kinetics across a dodecanethiol monolayer self-assembled on gold. *J. Electroanal. Chem.* 542: 7-11.